Appendix A. **Linear SDOF System**

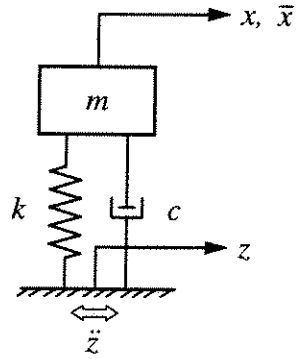

Figure A.1 SDOF system

Figure A.1 shows a SDOF system subjected to a base excitation. The equation of motion of the system is written as

$$m\ddot{\bar{x}} + c\dot{\bar{x}} + k\bar{x} = -m\ddot{z} \qquad \text{(A. 1)}$$

where m, k and c indicate the mass, stiffness and damping coefficients of the damper respectively; x and $\bar{x}$ are the absolute and relative displacements of the damper, respectively; z is the displacement of the base. In the next section, Equation (A.1) is solved using the frequency response analysis.

A.1 Frequency response analysis

The frequency response function is a frequency sweep series of the amplitude ratios and phase angles between the input and output functions which is useful to describe the dynamic characteristics of a linear system. If the base excitation is a harmonic function of a constant amplitude z_0 and fixed angular frequency ω

$$z = z_0 e^{i\omega t} \qquad \text{(A. 2)}$$

then, the steady state response of the system must also be a harmonic function of fixed amplitude $\bar{x}_0$ and the same frequency ω and phase difference ϕ, so that

$$\bar{x} = \bar{x}_0 e^{i(\omega t - \phi)}. \qquad \text{(A. 3)}$$

The complex frequency response functions relating $\bar{x}$ or x to z are respectively

$$H_{\bar{x}/z} = \frac{m\omega^2}{-m\omega^2 + k + ic\omega} = \frac{\beta^2}{1 - \beta^2 + i2\zeta\beta} \qquad \text{(A. 4)}$$

and $$H_{x/z} = 1 + H_{\bar{x}/z} = \frac{1 + i2\zeta\beta}{1 - \beta^2 + i2\zeta\beta} \quad \text{(A. 5)}$$

in which the excitation frequency ratio β and the damping ratio of the system ζ are defined as $\beta = \omega/\omega_s$ and $\zeta = c/2\sqrt{mk}$, respectively. The magnitude of $H_{x/z}$ and the phase angle ϕ between x and z are expressed respectively as

$$\left|H_{x/z}\right| = \sqrt{\frac{1 + (2\zeta\beta)^2}{(1-\beta^2)^2 + (2\zeta\beta)^2}} \quad \text{(A. 6)}$$

and $$\phi = \tan^{-1}\left(\frac{2\zeta\beta^3}{1 - \beta^2 + (2\zeta\beta)^2}\right). \quad \text{(A. 7)}$$

The magnitude of $H_{\bar{x}/z}$ is determined by

$$\left|H_{\bar{x}/z}\right| = \frac{\beta^2}{\sqrt{(1-\beta^2)^2 + (2\zeta\beta)^2}}. \quad \text{(A. 8)}$$

The frequency response function relating $\bar{x}$ to the excitation force F_e is determined by

$$H_{\bar{x}/F_e} = H_{\bar{x}/m\omega^2 z} = \frac{1}{k\beta^2} H_{\bar{x}/z}. \quad \text{(A. 9)}$$

The dynamic magnification factor (DMF) at the given excitation frequency and the corresponding amplitude of structural displacement are calculated respectively as

$$DMF = \frac{k}{F_0} x_0 = k\left|H_{\bar{x}/F_e}\right| = \frac{1}{\beta^2}\left|H_{\bar{x}/z}\right| = \frac{1}{\sqrt{(1-\beta^2)^2 + (2\zeta\beta)^2}} \quad \text{(A. 10)}$$

and $$x_0 = \frac{F_0}{k}\frac{1}{\sqrt{(1-\beta^2)^2 + (2\zeta\beta)^2}}. \quad \text{(A. 11)}$$

Note that F_0 is the amplitude of the excitation force. The maximum DMF and the corresponding amplitude of the structural displacement over the sweep excitation frequencies are obtained respectively by

$$DMF_{\max} = \frac{1}{2\zeta\sqrt{1-\zeta^2}} \tag{A. 12}$$

and

$$x_{0,\max} = \frac{F_0}{k}\frac{1}{2\zeta\sqrt{1-\zeta^2}} \tag{A. 13}$$

Figure A.2 shows the plots of Equation (A.6), (A.7) and (A.10) for the systems with various damping values.

A.2 Energy dissipation per cycle by a SDOF damping device

Suppose the SDOF system in Figure A.1 is a damping device which is subjected to a harmonic base excitation. The damping force F_d which is defined as the force resisting the base excitation is expressed as

$$F_d = -(c\dot{\bar{x}} + k\bar{x}). \tag{A. 14}$$

Noting $-(c\dot{\bar{x}} + k\bar{x}) = m\ddot{x}$ from Equation (A.1), F_d can be calculated by

$$F_d = -(c\dot{\bar{x}} + k\bar{x}) = m\ddot{x} = -m\omega^2 x = -m\omega^2 z_0 \left|H_{x/z}\right| e^{i(\omega t-\phi)}. \tag{A. 15}$$

Dividing by $m\ddot{z}_0 = -m\omega^2 z_0$, the nondimensional amplitude of the damping force F_d' becomes

$$\left|F_d'\right| = \left|H_{x/z}\right| = \sqrt{\frac{1+(2\zeta\beta)^2}{(1-\beta^2)^2+(2\zeta\beta)^2}}. \tag{A. 16}$$

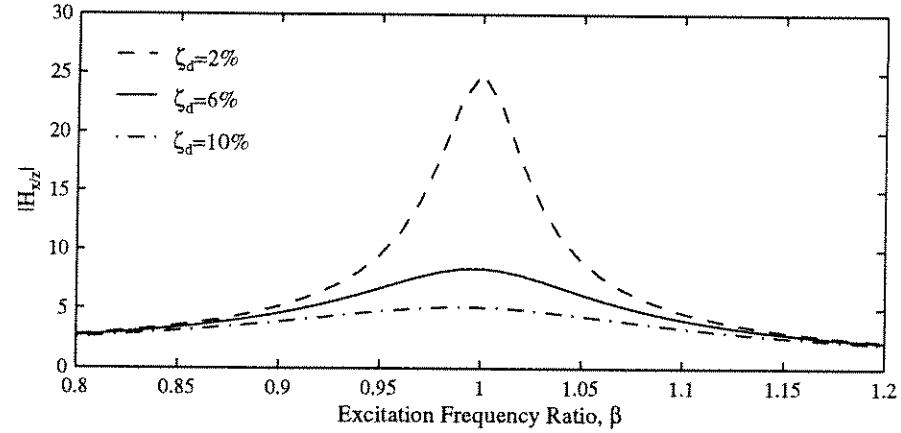

(a) Amplitude of frequency response function

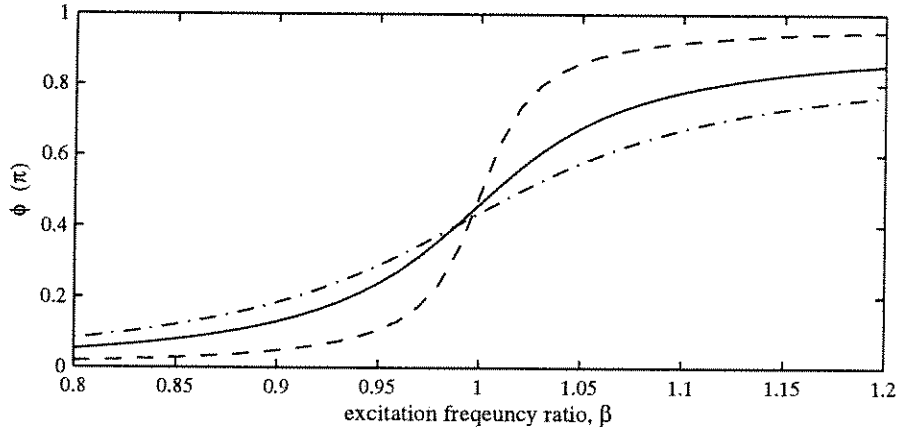

(b) Phase angle

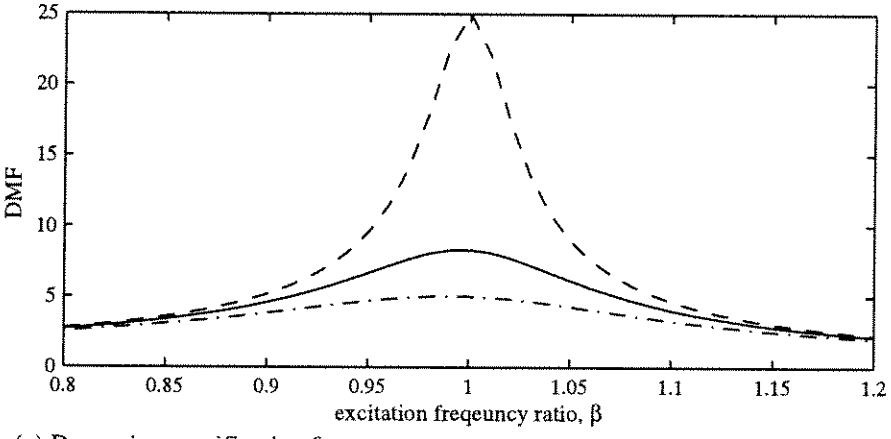

(c) Dynamic magnification factor

Figure A.2 Frequency responses of SDOF systems with various damping values calculated using Equations (A.6), (A.7) and (A.10).

The energy dissipation by the damper E_d is defined as the amount of work done by the damping forces during one cycle of the base excitation and calculated by

$$E_d = \int_{cycle} F_d dz = \int_T F_d \dot{z} dt = -m\omega^3 z_0^2 \left| H_{x/z} \right| \int_0^T (e^{i(\omega t - \phi)})(ie^{i\omega t}) dt \,. \qquad \text{(A. 17)}$$

Assuming a sine wave input, i.e., $z = z_0 \,\mathrm{Im}(e^{i\omega t}) = z_0 \sin(\omega t)$, Equation (A.17) is rewritten as

$$E_d = -m\omega^3 z_0^2 \left| H_{x/z} \right| \int_0^T (\sin(\omega t - \phi)\cos \omega t) dt = -m\omega^2 z_0^2 \pi \left| H_{x/z} \right| \sin\phi \,. \qquad \text{(A. 18)}$$

Dividing by $-\frac{1}{2} m(\omega z_0)^2$, it is written in the nondimensional form as,

$$E_d' = 2\pi \left| H_{x/z} \right| \sin\phi \xrightarrow{or} E_d' = 2\pi \left| F_d' \right| \sin\phi \,. \qquad \text{(A. 19)}$$

Figure A.3(a) presents the sweep frequency plots of the nondimensional energy dissipation calculated using Equation (A.19) for dampers with various damping values. The damper with lower damping ratio shows the higher and narrower energy dissipation curve. The influence of the damper stiffness on the energy dissipation capacity is illustrated on Figure A.3(b). The solid line is the frequency sweep plot of the energy dissipation capacity of a SDOF system with the damping ratio of 6 % and an arbitrary natural frequency, f_{d1}. The system's natural frequency is increased by 5% and 10% respectively by increasing the stiffness of the system by 10.25% and 21% respectively. The frequency shifting ratio ξ is defined as the ratio of the natural frequency of each system to that of the original system. Hence, ξ values of three systems shown on the figure are 1.0, 1.05 and 1.10 respectively. The x-axis of the plot is the ratio of the excitation frequency to the natural frequency of the original system of which ξ = 1.0. As the natural frequency of the system is increased the energy dissipation curve for the system shifts toward higher β region. The observed trends of the influences of damping and

stiffness of the system on the energy dissipation capacity is utilized in searching for an equivalent mechanical model of each TLD.

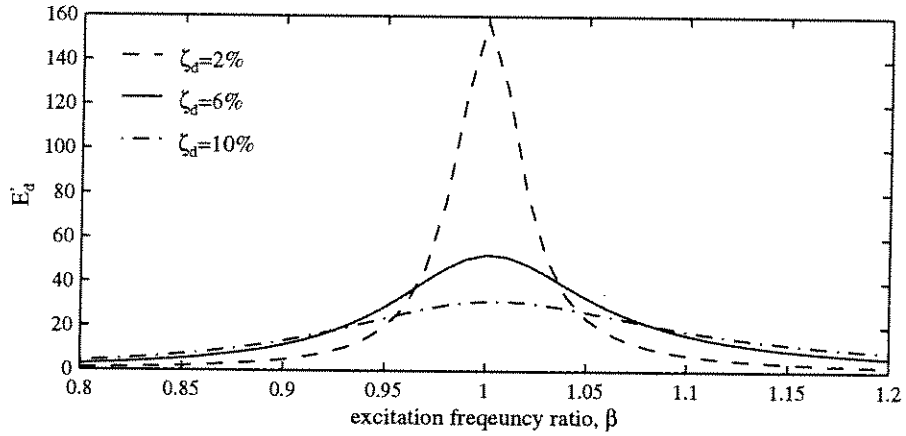

(a) with various damping values

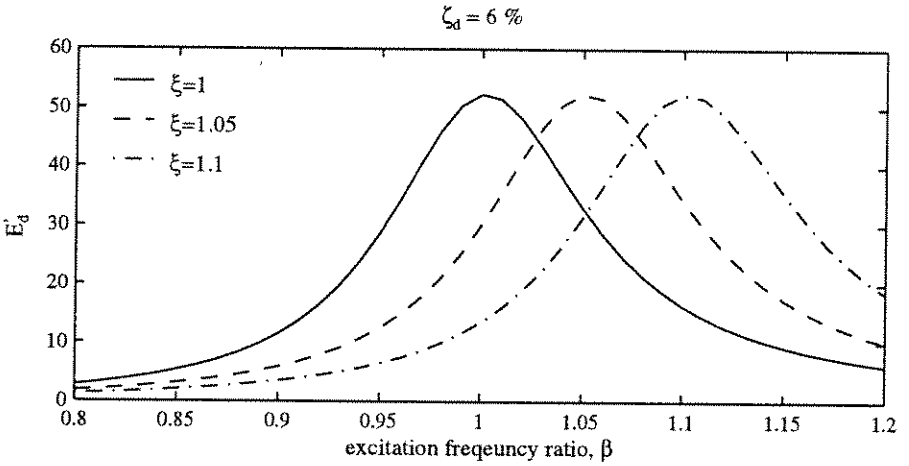

(b) with various stiffness values

Figure A.3 Energy dissipation curves for SDOF systems with various damping or various stiffness values. Calculated using Equation (A.19).

Appendix B. **Linear 2DOF System under Harmonic Excitation***

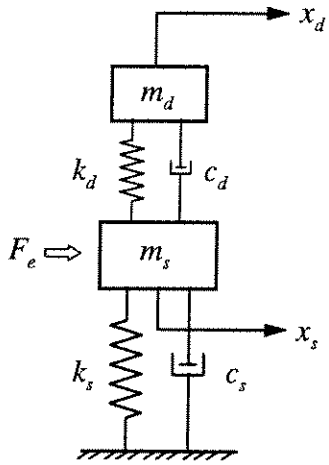

Figure B.1 SDOF structure with a damper

A SDOF structure with a SDOF mechanical damper is modeled as a simple linear two degree of freedom system as shown in Figure B.1. In Section B.1, the frequency response function of the system is derived. The steady state responses of undamped or lightly damped structures under harmonic excitation force are calculated using the frequency response function. The well-known optimal parameters of the TMD attached to an undamped or a lightly damped structure are briefly reviewed in Section B.2. The behavior and performance of the TMDs with various damping values are illustrated in Section B.3.

For the 2DOF system shown on Figure B.1, the equations of motion are written as

$$\begin{bmatrix} m_d & 0 \\ 0 & m_s \end{bmatrix}\begin{Bmatrix} \ddot{x}_d \\ \ddot{x}_s \end{Bmatrix}+\begin{bmatrix} c_d & -c_d \\ -c_d & c_d+c_s \end{bmatrix}\begin{Bmatrix} \dot{x}_d \\ \dot{x}_s \end{Bmatrix}+\begin{bmatrix} k_d & -k_d \\ -k_d & k_d+k_s \end{bmatrix}\begin{Bmatrix} x_d \\ x_s \end{Bmatrix}=\begin{Bmatrix} 0 \\ F_e \end{Bmatrix}. \qquad \text{(B. 1)}$$

B.1 Frequency response analysis

As a structure is subjected to a harmonic excitation, the external force and the steady-state response of the structure can be expressed respectively as

$$F_e = F_0 e^{i\omega t} \quad and$$
$$x_s = x_0 e^{i(\omega t-\phi)}. \qquad \text{(B. 2)}$$

* See "List of Symbol" for the definition of the variables which are not defined in this section.

Introducing the parameters

$$\omega_s = \sqrt{\frac{k_s}{m_s}},\ \omega_d = \sqrt{\frac{k_d}{m_d}},\ \zeta_s = \frac{c_s}{2\sqrt{k_s m_s}},\ \zeta_d = \frac{c_d}{2\sqrt{k_d m_d}},$$

$$\mu = \frac{m_d}{m_s},\ \beta = \frac{\omega}{\omega_s},\ \beta_d = \frac{\omega}{\omega_d},\ \text{and}\ \ \gamma = \frac{\omega_d}{\omega_s} = \frac{\beta}{\beta_d}, \tag{B. 3}$$

the complex frequency response function relating x_s to F_e can be obtained by

$$H_{x_s} = H_{x_s/F_e} = \frac{1}{k_s\left(1-\beta^2 + i2\zeta_s\beta - \mu\beta^2 H_{x_d}\right)} \tag{B. 4}$$

where the complex frequency response function relating x_d to x_s is

$$H_{x_d} = H_{x_d/x_s} = \frac{1+i2\zeta_d\beta_d}{1-\beta_d{}^2 + i2\zeta_d\beta_d} = \frac{\gamma^2\left(\gamma^2-\beta^2+\left(2\zeta_d\beta\right)^2\right)-i2\gamma\zeta_d\beta^3}{\left(\gamma^2-\beta^2\right)^2+\left(2\gamma\zeta_d\beta\right)^2}. \tag{B. 5}$$

Substituting (B.5) and after some manipulations, Equation (B.4) becomes

$$H_{x_s} = \frac{1}{k_s}\frac{1}{RE + iIM} \tag{B. 6}$$

where

$$RE = 1-\beta^2 - \mu\beta^2\frac{\gamma^2\left(\gamma^2-\beta^2+\left(2\zeta_d\beta\right)^2\right)}{\left(\gamma^2-\beta^2\right)^2+\left(2\gamma\zeta_d\beta\right)^2}\ \ \textit{and}$$
$$IM = 2\zeta_s\beta + \frac{2\mu\gamma\zeta_d\beta^5}{\left(\gamma^2-\beta^2\right)^2+\left(2\gamma\zeta_d\beta\right)^2}. \tag{B. 7}$$

The dynamic magnification factor (DMF) and its corresponding peak displacement of the structure at the given excitation frequency are obtained respectively by

$$DMF = \frac{k_s}{F_0}x_0 = k_s\left|H_{x_s}\right| = \frac{1}{\sqrt{RE^2+IM^2}}\ \ \text{and} \tag{B. 8}$$

$$x_0 = \frac{F_0}{k_s} \frac{1}{\sqrt{RE^2 + IM^2}} \,. \tag{B. 9}$$

The normalized peak displacement of the structure at the given excitation frequency is defined as

$$x_0' = \frac{x_0}{x_{0,\max}} = \frac{2\zeta_s \sqrt{1-\zeta_s^2}}{\sqrt{RE^2 + IM^2}} \tag{B. 10}$$

where $x_{0,\max}$ is the maximum peak displacement of the structure without a damper over the sweep excitation frequencies which is expressed in Equation (A.13).

B.2 Optimum design parameters of the linear mechanical damper

Undamped Structure, $\zeta_s = 0$: Substituting $\zeta_s = 0$ into (B.7) and (B.9), the familiar Den Hartog's expression (Den Hartog, 1954) is obtained. Following the well-known procedure utilizing the existence of invariant points on the response curves, we can obtain the optimum tuning ratio and optimum damping ratio of the damper as follows,

$$\gamma_{opt} = \frac{1}{1+\mu} \quad and$$
$$\zeta_{d,opt} = \sqrt{\frac{3\mu}{8(1+\mu)}} \,. \tag{B. 11}$$

Lightly Damped Structure, $\zeta_s > 0$: For the system with a damped structure, the invariant points do not exist anymore in the response curves. The optimum parameters of the damper cannot be obtained using the analytical method as for the undamped case. The optimum parameters of the damper for the system with a damped structure can be determined by a numerical search for the minimum peak response, e.g., Warburton (1980) and Tsai (1993). For the lightly damped structure ($\zeta_s \le 0.01$) subjected to harmonic excitation, the optimum parameters of the damper were found to be

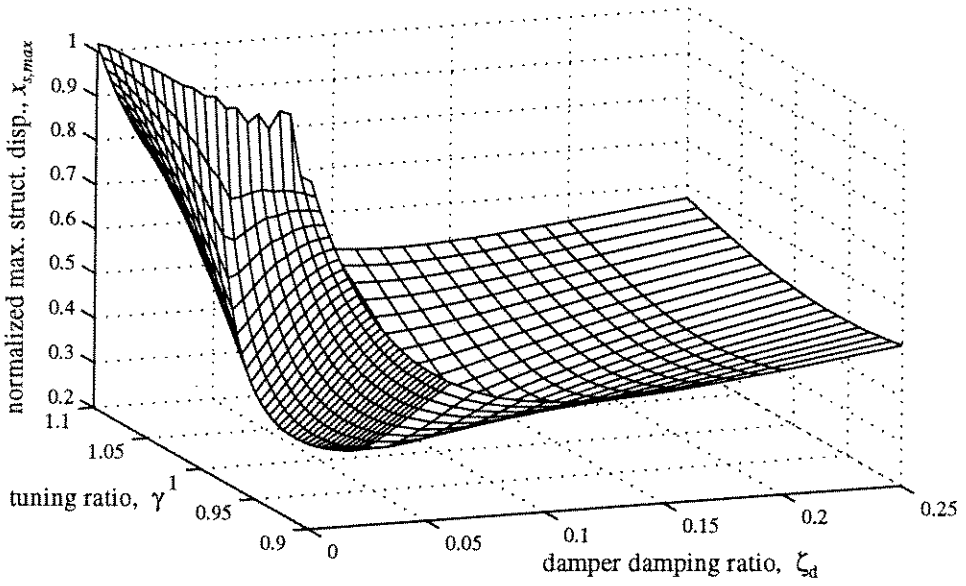

Figure B.2 Normalized peak displacements of the structure equipped with a TMD for harmonic excitation: The structural damping ratio, ζ_s=1.0 %. The mass ratio, μ=1.0 %.

$$\gamma_{opt} \approx 0.99$$
$$\zeta_{d,opt} \approx 0.06 \qquad \text{(B. 12)}$$

Figure B.2 containes a 3-D plot of the normalized peak displacements of a structure equipped with various TMDs for the structural damping ratio ζ_s = 1.0 % and the damper mass ratio μ = 1.0 %. The tuning ratios γ vary in the range between 0.9 and 1.1 in the increment of 0.01. The optimum parameters for the damper as defined in Equation (B.12) are evident in this figure.

B.3 Performance of the TMD - Case study

Figure B.3 shows the frequency response plots of a lightly damped structure with three differently damped TMDs under harmonic external force. The mass ratio μ of each TMD is 1%. The structural damping ratio ζ_s is 0.7%.

For the given system, the optimum parameters were found as in Equation (B.12). In these analyses, the TMDs are tuned to the fundamental natural frequency of the structure. The damping ratios of each TMD ζ_d are 2 % (under-damped), 6 % (optimally damped) and 20 % (over-damped) respectively. The dynamic magnification factor (DMF) of each system was calculated using Equation (B.8). The figure identifies that the optimally-damped TMD reduces the peak displacement of the structure most effectively over the broad range of the excitation frequencies.

Figure B.4 shows the time history performances of each TMD under the free vibration of the structure with the initial displacement x_0 = 50 mm. The structural motion shows a beating phenomenon with the under-damped TMD. In general, as the damping of the TMD approaches the optimal value, the beating phenomenon weakens and finally

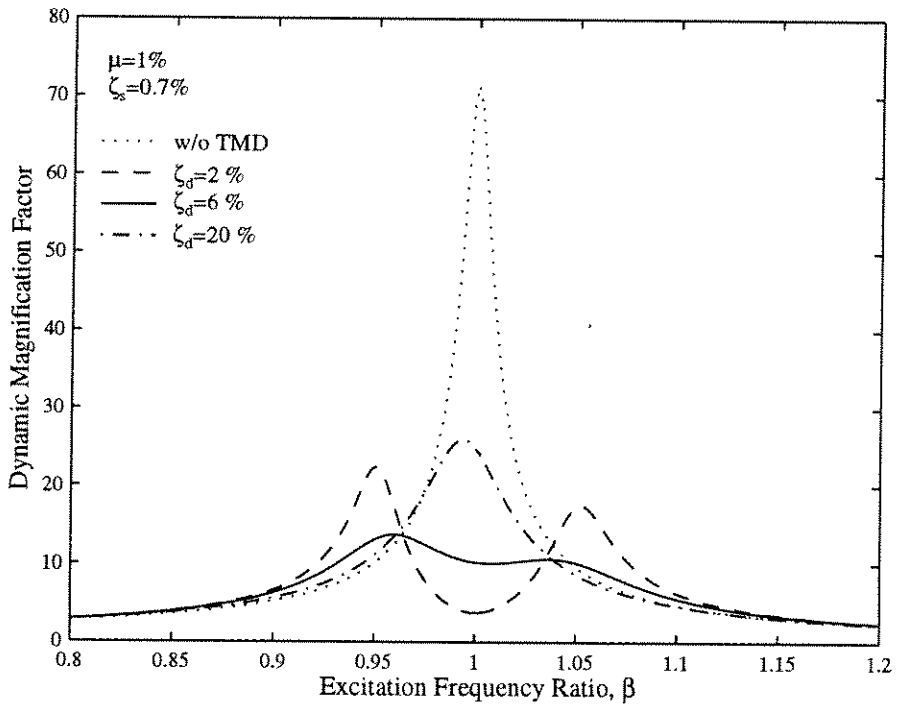

Figure B.3 Frequency response of lightly damped structures with variously damped TMDs

disappears near the optimal value. If the damping of the TMD keeps increasing beyond the optimal value, the structural motion decays more slowly.

Figure B.5 shows the time history responses of a structure with the same TMDs under harmonic excitation at excitation frequency ratio β of 1.0 and 0.95 respectively. The amplitude of the external force was selected such that the maximum displacement of the structure without TMD became 50 mm under the given forcing function. Near the vicinity of the excitation frequency ratio of unity (i.e., the β = 1.0), the under-damped TMD (ζ_d = 2%) reduces the structural response most effectively. But the under-damped TMD performs worst at β = 0.95. The behavior of the over-damped TMD is opposite to that of the under-damped TMD. The optimally-damped TMD performs effectively over the broad range of the excitation frequencies. These observations are consistent with the plots in Figure B.4.

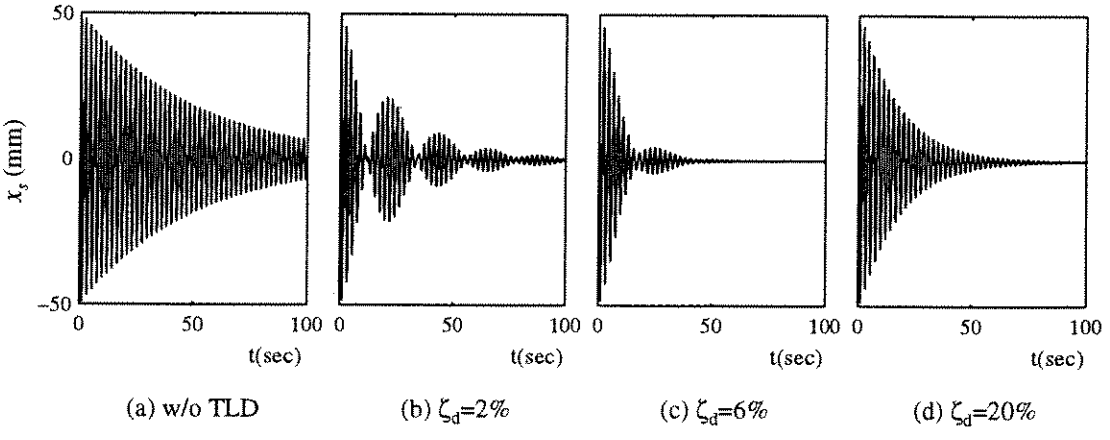

Figure B.4 Time history free vibration responses of lightly damped structures with variously damped TMDs under harmonic excitation

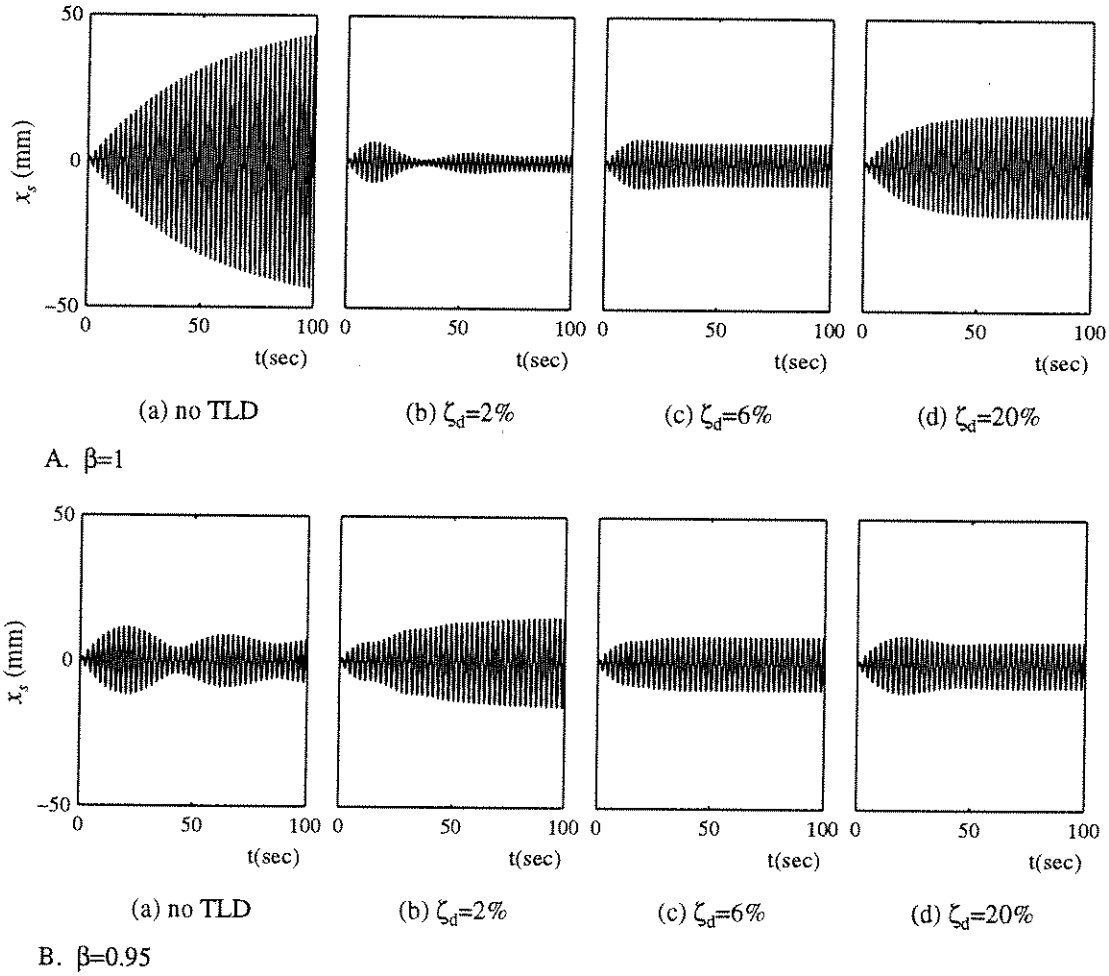

Figure B.5 Time history forced vibration responses of lightly damped structures with variously damped TMDs under harmonic excitation

Appendix C. **Linear 2DOF System under White Noise Excitations** *

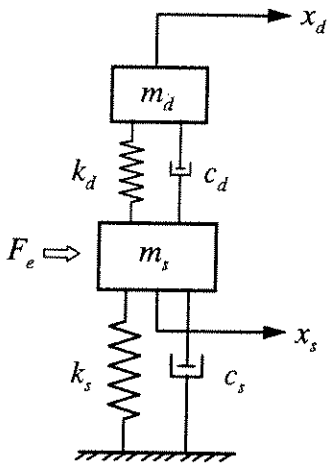

Figure C.1 SDOF structure with a damper

Figure C.1 shows a simple linear two degree of freedom system subjected to an external force. If the external force is random with a constant spectral density (white noise spectrum), the steady state response of the stationary process can be obtained. In Section C.1, the steady state response of the system is calculated using frequency response analysis coupled with spectral analysis. The optimal parameters of the TMD attached to an undamped or lightly damped structure are briefly reviewed in Section C.2.

C.1 Steady state responses

To obtain the steady-state response of the system under a random excitation with a constant spectral density S_0, the frequency response functions, H_{x_s} and H_{x_d} in Equations (B.4) and (B.5) are rewritten respectively as

$$H_{x_s} = \frac{1}{m_s(i\omega)^2 + c_s(i\omega) + k_s + m_d H_{x_d}(i\omega)^2} \quad \text{and} \tag{C.1}$$

$$H_{x_d} = \frac{k_d + c_d(i\omega)}{k_d + c_d(i\omega) + m_d(i\omega)^2} \,. \tag{C.2}$$

Substituting (C.2) into (C.1) and after some manipulations using (B.3), we obtain

* See "List of Symbol" for the definition of the variables which are not defined in this section.

$$H_{x_s} = \frac{1}{m_s} \frac{B_0 + B_1(i\omega) + B_2(i\omega)^2 + B_3(i\omega)^3}{A_0 + A_1(i\omega) + A_2(i\omega)^2 + A_3(i\omega)^3 + A_4(i\omega)^4} \tag{C.3}$$

where

$$\begin{aligned} A_0 &= {\omega_s}^2 {\omega_d}^2; \quad A_1 = 2\zeta_s \omega_s {\omega_d}^2 + 2\zeta_d {\omega_s}^2 \omega_d; \\ A_2 &= 4\zeta_s \zeta_d \omega_s \omega_d + {\omega_s}^2 + {\omega_d}^2 (1+\mu); \\ A_3 &= 2\zeta_s \omega_s + 2\zeta_d \omega_d (1+\mu); \quad A_4 = 1; \\ B_0 &= {\omega_d}^2; \quad B_1 = 2\zeta_d \omega_d; \quad B_2 = 1; \quad B_3 = 0. \end{aligned} \tag{C.4}$$

The mean square response of a stationary response process is given by

$$E\left[{x_s}^2\right] = S_0 \int_{-\infty}^{\infty} \left| H_{x_s}(\omega) \right|^2 d\omega. \tag{C.5}$$

Substituting (C.3) into (C.5) and evaluating the integral (Newland, 3rd ed., pp.372), the mean square response is obtained in the form

$$E\left[{x_s}^2\right] = \frac{\pi S_0}{{m_s}^2} \Pi(A_0, \cdots, A_4, B_0, \cdots, B_s) \tag{C.6}$$

in which

$$\Pi = \frac{\begin{array}{c} A_0 {B_3}^2 (A_0 A_3 - A_1 A_2) + A_0 A_1 A_4 (2B_1 B_3 - {B_2}^3) \\ -A_0 A_3 A_4 ({B_1}^2 - 2B_0 B_2) + A_4 {B_0}^2 (A_1 A_4 - A_2 A_3) \end{array}}{A_0 A_4 (A_0 {A_3}^2 + {A_1}^2 A_4 - A_1 A_2 A_3)}. \tag{C.7}$$

Substituting A_4=1, B_2=1 and B_3=0, it is simplified as

$$\Pi = \frac{-A_0 A_1 - A_0 A_3 ({B_1}^2 - 2B_0) + {B_0}^2 (A_1 - A_2 A_3)}{A_0 (A_0 {A_3}^2 + {A_1}^2 - A_1 A_2 A_3)}. \tag{C.8}$$

Introducing new variables

$$\overline{A}_i = \frac{A_i}{\omega_s^{4-i}}; \quad \overline{B}_i = \frac{B_i}{\omega_s^{2-i}}; \tag{C.9}$$

i.e.,

$$\begin{gathered}\overline{A}_0 = \gamma^2; \quad \overline{A}_1 = 2(\zeta_s\gamma^2 + \zeta_d\gamma); \quad \overline{A}_2 = 4\zeta_s\zeta_d\gamma + 1 + \gamma^2(1+\mu); \\ \overline{A}_3 = 2(\zeta_s + \zeta_d(1+\mu)\gamma); \quad \overline{B}_0 = \gamma^2 = \overline{A}_0; \quad \overline{B}_1 = 2\zeta_d\gamma,\end{gathered} \tag{C.10}$$

Equation (C.8) is simplified as

$$\Pi = \frac{1}{\omega_s^3}\overline{\Pi} \tag{C.11}$$

where, $$\overline{\Pi} = \frac{-\overline{A}_1 - \overline{A}_3(\overline{B}_1^2 - 2\overline{A}_0) + \overline{A}_0(\overline{A}_1 - \overline{A}_2\overline{A}_3)}{\overline{A}_0\overline{A}_3^2 + \overline{A}_1^2 - \overline{A}_1\overline{A}_2\overline{A}_3}. \tag{C.12}$$

Equation (C.6) is rewritten as

$$E\left[x_s^2\right] = \frac{\pi S_0}{m_s^2\omega_s^3}\overline{\Pi}. \tag{C.13}$$

Mean square response of the structure without damper can be obtained by

$$E\left[x_{s,0}^2\right] = \frac{\pi S_0}{2\zeta_s m_s^2\omega_s^3}. \tag{C.14}$$

Normalizing (C.13) to (C.14), the nondimensional mean square response of the structure is written as

$$E'\left[x_s^2\right] = \frac{E\left[x_s^2\right]}{E\left[x_{s,0}^2\right]} = 2\zeta_s\overline{\Pi} \tag{C.15}$$

which is a function of μ, ζ_s, ζ_d and γ.

C.2 Optimum design parameters for the linear mechanical damper

The optimum parameters for the damper can be determined through numerical searches for the minimum peak response by solving Equation (C.15). An extensive numerical search for the optimum parameters has been conducted and reported by Warburton (1982). Figure C.2 shows the plots for the normalized RMS displacement of a structure equipped with various TMDs as the structural damping ratio ζ_s = 1.0 % and the damper mass ratio μ = 1.0 %. The tuning ratio γ vary in the range between 0.9 and 1.1 with the increment of 0.01. The damper damping ratios ζ_d range from to 0.25. For the given structure, the optimum parameters were identified from the figure as

$$\gamma_{opt} \approx 0.99 \quad and$$
$$\zeta_{d,opt} \approx 0.05. \tag{C.16}$$

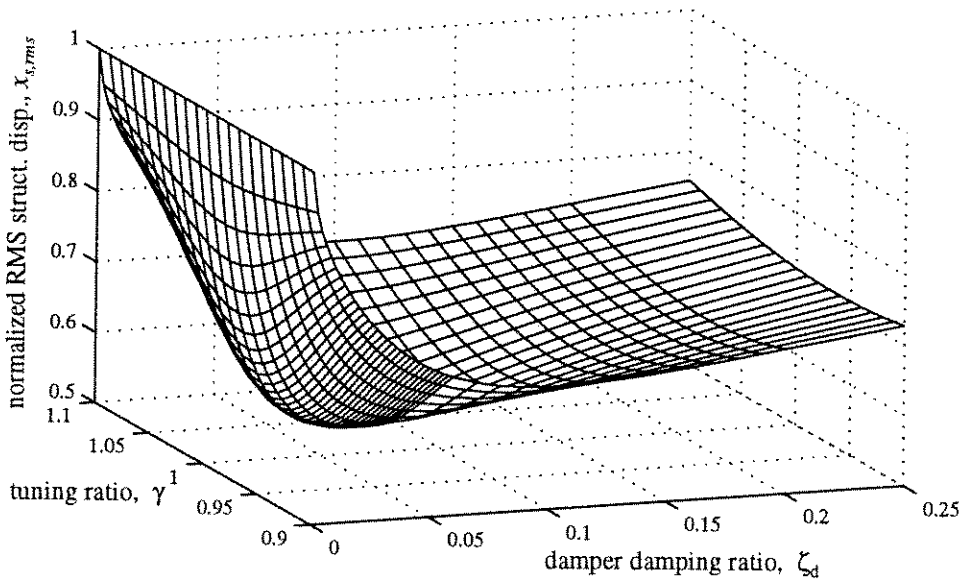

Figure C.2 Normalized RMS displacements of the structure equipped with a TMD for white noise excitation: The structural damping ratio, ζ_s=1.0%. The mass ratio, μ=1.0%.

Appendix D. **Time history analysis for a SDOF structure equipped with a TLD under an arbitrary excitation.**

As a SDOF structure equipped with a TLD is subjected to an arbitrary external force, the equation of motion is written as

$$m\ddot{x} + c\dot{x} + kx = F_e + F_d \tag{D. 1}$$

where m, c and k indicate the mass, damping and stiffness coefficients of the structure respectively; x indicates the relative displacement of the structure; F_e is the excitation forcing function; and F_d is the hydrodynamic force induced by water sloshing motion in the TLD.

In the numerical time history analysis of the structural response to the driving force, the external force is approximated as a piecewisely constant step function. At each time step, Equation (D.1) can be rewritten in the form

$$m\ddot{x}_i + c\dot{x}_i + kx_i = P_i \ . \tag{D. 2}$$

If the displacement and the velocity of the structure at time step t_{i-1} are known, i.e., x_{i-1} *and* $\dot{x}_{i-1}$ are known, the responses at the time step t_i can be obtained by solving Equation (D.2). The results are as follows:

$$x_i = e^{-\zeta\omega\Delta t}(A\sin\omega_d\Delta t + B\cos\omega_d\Delta t) + \frac{P_i}{k} \ , \tag{D. 3}$$

$$\dot{x}_i = -\zeta\omega e^{-\zeta\omega\Delta t}(A\sin\omega_d\Delta t + B\cos\omega_d\Delta t) + e^{-\zeta\omega\Delta t}\omega_d(A\cos\omega_d\Delta t - B\sin\omega_d\Delta t) \ , \tag{D. 4}$$

and

$$\ddot{x}_i = e^{-\zeta\omega\Delta t}[((2\zeta^2-1)\omega^2 A + 2\zeta\omega\omega_d B)\sin\omega_d\Delta t + ((-2\zeta\omega\omega_d A + (2\zeta^2-1)\omega^2 B)\cos\omega_d\Delta t] \tag{D. 5}$$

where, ζ and ω are the damping ratio and the natural angular frequency of the structure respectively and $\omega_d = \omega\sqrt{1-\zeta^2}$. At time step t_{i-1}, substitute $\Delta t = 0$ and we obtain

$$x_{i-1} = B + \frac{P_i}{k} \quad \Rightarrow \quad B = x_{i-1} - \frac{P_i}{k} \tag{D. 6}$$

and $$\dot{x}_{i-1} = -\zeta\omega B + \omega_d A \quad \Rightarrow \quad A = \frac{1}{\omega_d}(\dot{x}_{i-1} + \zeta\omega(x_{i-1} - \frac{P_i}{k})). \tag{D. 7}$$

Substituting (D.6) and (D.7) into (D.3), (D.4) and (D5) and noticing $t = \Delta t$ at time step t_i, we obtain displacement, velocity and acceleration at current time step. This numerical scheme is employed to solve the dynamic equations of motion for the SDOF system with TLD as the TLD is modeled with a fluid model.

Appendix E. **The Results for the Shaking Table Experimental Investigations.**

The data and results of the energy dissipation matching procedure for the experimental cases of rectangular tanks, which are plotted in Figure 3.3, are tabulated in Table E.1. Those for numerical simulation using the random choice method, which

Table E.1: The data and results for the rectangular tanks.

Tank Size		*Water*	*Excitation Amplitude*		*NSD Model*	
Length L *(mm)*	Width b *(mm)*	Depth h_0 *(mm)*	A *(mm)*	A/L	ζ_d	κ
590	335	15	10	0.017	0.16	1.02
			20	0.034	0.22	1.08
			40	0.068	0.23	1.35
590	335	22.5	10	0.017	0.12	1.08
			20	0.034	0.15	1.08
			40	0.068	0.20	1.32
590	335	30	10	0.017	0.11	1.10
			20	0.034	0.15	1.06
			40	0.068	0.22	1.25
590	335	45	20	0.034	0.17	1.10
900	335	40	2.5	0.003	0.08	1.00
			5	0.006	0.09	1.10
			10	0.011	0.10	1.12
			20	0.022	0.15	1.02
			20	0.022	0.16	1.02
			30	0.033	0.18	1.04
			40	0.044	0.20	1.15
900	335	55	20	0.022	0.13	1.08
335	203	15	2.5	0.007	0.09	1.02
			2.5	0.007	0.07	1.00
			5	0.015	0.11	1.02
			5	0.015	0.10	1.00
			10	0.030	0.15	1.04
			10	0.030	0.14	1.04
			20	0.060	0.18	1.21
			20	0.060	0.17	1.25
			30	0.090	0.20	1.32

correspond to Figure 3.7, are tabulated in Table E.2. Table E.3 summarizes those for experimental cases of circular tanks, which are plotted in Figure 3.4.

Table E.2. The data and results for the rectangular TLDs obtained from the numerical simulation using the RCM model.

Tank Size		*Water*	*Excitation Amplitude*		*NSD Model*	
Length L *(mm)*	*Width* b *(mm)*	*Depth* h_0 *(mm)*	A *(mm)*	A/L	ζ_d	κ
590	335	30	10	0.017	0.11	1.04
			20	0.034	0.14	1.10
			30	0.051	0.18	1.12
			40	0.068	0.21	1.15
900	335	40	10	0.011	0.10	1.02
			20	0.022	0.13	1.04
			30	0.033	0.16	1.06
			40	0.044	0.17	1.08

Table E.3. The data and results for the circular tanks.

Tank Size	*Water*	*Excitation Amplitude*		*NSD Model*	
Diameter D *(mm)*	*Depth* h_0 *(mm)*	A *(mm)*	A/L	ζ_d	κ
690	15	10	.017	0.14	1.00
		20	.034	0.20	1.12
		40	.068	0.23	1.30
	22.5	10	.017	0.15	1.00
		20	.034	0.19	1.15
		40	.068	0.23	1.32
690	30	2.5	.004	0.06	1.06
		5	.008	0.07	1.15
		10	.017	0.15	1.15
		20	.034	0.19	1.18
		30	.051	0.16	1.23
		40	.068	0.19	1.35
	45	5	.008	0.07	1.00
		10	.017	0.10	1.04

Appendix F. **Shallow-Water Wave Theory**

Assuming an inviscid incompressible fluid in a constant gravitational field, the laws of mass conservation and momentum conservation give

$$\nabla \cdot \vec{q} = 0 \tag{F.1}$$

$$\rho(\vec{q}_t + \vec{q} \cdot \nabla \vec{q}) = -\nabla(p + \rho g y) \tag{F.2}$$

where $\vec{q} = u\vec{i} + v\vec{j} + w\vec{k}$ is the velocity vector in which $\vec{i}$, $\vec{j}$, $\vec{k}$ are the cartesian unit vectors along axes x, y and z, respectively, p is the pressure, ρ is the fluid density and g is the acceleration of gravity.

Consider the two-dimensional flow as shown on Figure F.1 by assuming that the velocity field is independent of z-axis (the lateral direction). Equation (F.1) can be rewritten as

$$u_x + v_y = 0 \tag{F.3}$$

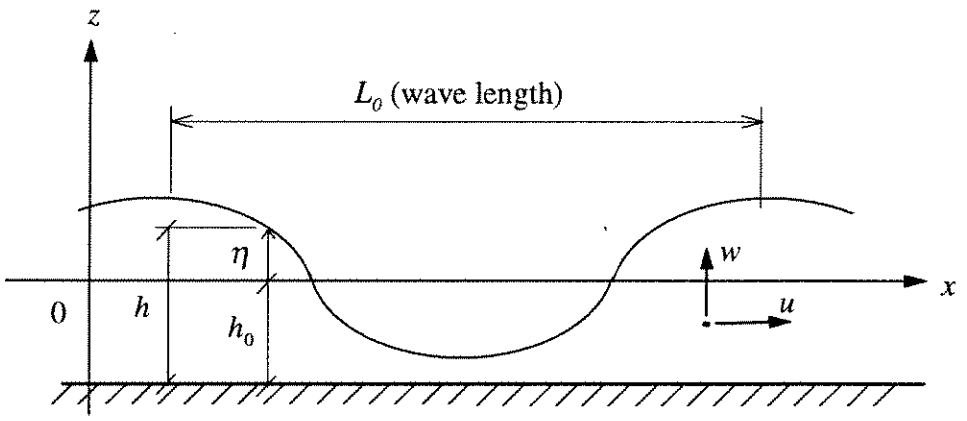

Figure F.1 Geometry of the shallow water wave

Integration of (F.3) over the water depth, $y = -h_0$ to η, leads to

$$\int_{-h_0}^{\eta} (u_x + v_y)dy = \frac{\partial}{\partial x}\int_{-h_0}^{\eta} udy + [v]_{y=-h_0}^{y=\eta}[u]_{y=\eta}\eta_x - [u]_{y=-h_0}h_{0,x} = 0 \qquad \text{(F.4)}$$

For a flat horizontal bottom, $h_{0,x} = 0$ and the last term disappears. Now introducing the kinematic boundary conditions at the bottom and the free surface

$$v = \eta_t + u\eta_x \quad \text{on the free surface, } y = \eta \qquad \text{(F.5)}$$

$$v = 0 \quad \text{on the bottom, } y = -h_0 \qquad \text{(F.6)}$$

Equation (F.4) is simplified as

$$\frac{\partial}{\partial x}\int_{-h_0}^{\eta} udy + \eta_t = 0 \qquad \text{(F.7)}$$

Noticing the disturbed water depth, $h = \eta + h_0$ hence $h_t = \eta_t$ and u is constant over the water depth, equation (F.7) can be rewritten as the final form

$$h_t + (uh)_x = 0 \qquad \text{(F.8)}$$

In hydrostatic pressure field, i.e., $p_y = -\rho g$ or, $p = \rho g(\eta - y)$, the momentum conservation in the horizontal direction from the equation (F.2) becomes

$$u_t + uu_x + vu_y = -g\eta_x \qquad \text{(F.9)}$$

Again, noticing $u_y = 0$ and $h_x = \eta_x$, the equation (F.9) becomes in the final form

$$u_t + uu_x + gh_x = 0 \qquad \text{(F.10)}$$

Equations (F.8) and (F.10) are the shallow-water wave equations. The wave motions based on the shallow-water wave equations are nondispersive and fully nonlinear.

VITA

Jin Kyu Yu

The author was born in Korea on August 7, 1957. He earned a Bachelor of Science degree in Architectural Engineering in January 1981 from Seoul National University in Seoul, Korea. After graduation he worked for five years as a field construction engineer for Dong Bu Construction Company.

He then came to U.S. to pursue an advanced degree in structural engineering. After graduating from Drexel University in June 1989 with a degree of Master of Science in Civil Engineering, he worked as a structural consulting engineer responsible for structural design of building structures.

In September 1993 he started his Ph.D. study at University of Washington in the Structural and Geotechnical Engineering and Mechanics Program of the Civil Engineering Department. He was interested in the field of structural vibration control and made his Ph.D. dissertation titled "Nonlinear Characteristics of Tuned Liquid Damper".

After graduation he plans to continue his practice in building design and apply his experience and knowledge of the structural vibration control to the practice.